Author's response to

Referee Comments 1 (Stephen M. Griffies)

1 Recommondation

This manuscript documents a new community diagnostic code for computing the diathermohaline circulation, both the stream function and the stream potential. It is a valuable contribution that is well written and well tested. I recommend publication after minor revisions.

We thank Stephen Griffies for thoroughly reviewing our manuscript, the positive feedback and constructive comments. We answer them in blue below and reference our manuscript changes with line numbers of the revised manuscript. Please note that, according to the comments, we updated the code as new version v2026.2 (Jung et al., 2026).

2 General comments

Why did you use Fortran (lines 51-52) rather than Python? Many community diagnostic codes are in Python, given it is more readily known and there are strong community diagnostic codes available in Python. The diagnostic working group for NEMO (I am co-chair) is organizing community diagnostic code, with nearly all code in Python. MOM5 and MOM6 diagnostic codes are also heavily biased to Python. Hence, I am very concerned that your choice to use Fortran will prove to be a barrier for community uptake of your diagnostic package. I strongly recommend writing and supporting a Python version!

Yes, this is a very good point. We plan to work on a Python version to make the computation for the diathermohaline stream function even more user friendly. For now, we would like to remain with the Fortran version to benefit from the compiled language performance. Possible future work could be a parallelized Python code or a version that is built on an interface between Fortran and Python to benefit from the Fortran performance.

3 Specific comments

- Line 11 of the abstract says that one can use the code for "any tracer coordinates". This is powerful and welcome. But there is no mention of any possible issues with the use of, say, carbon as a coordinate. I suggest this topic could form a useful part of the concluding section. It is a great feature that should be mentioned more.
  We are glad to hear that this function is welcome. We picked it up in Sect. 2.1, 2.2 and 7. However, including the interpretation of stream functions in other tracer spaces would exceed the scope of the paper.
  Manuscript changes: We added:
  - the lines 102-104: "It is worth noting, that throughout this work we use potential temperature θ and practical salinity S as variables for the tracer space. However, those variables can be replaced by conservative temperature and absolute salinity and also by other variables to define stream functions in other tracer spaces."
  - the lines: 151-153: "Please note, that the needed resolution might change in case other tracers are used and it is therefore recommended to verify in a similar resolution study whether the solution is robust to the chosen resolution."
  - the line 494-495: "[...] and can be also applied to other tracer spaces"
- Line 25: I suggest citing as "Walin (1977, 1982)" rather than "Walin in 1977 and 1982".
  Thank you. We changed it.

- Line 26: add “space” after “temperature”.
  Thank you. We changed it.

- Line 35: I suggest adding Zhang and Thomas (2021) for another example of “temperature-density”coordinate work, with particular focus on OSNAP.1.
  We added the reference.
  Manuscript changes: We added:
  - the lines 35-36: "[...] and which were for example used by Zhang and Thomas (2021) to study the AMOC transports."

- Lines 53-54: The authors claim to have “a more accurate projection of volume transports into thermohaline space.” This is great. But I did not see further mention of this potentially central technical detail. I recommend more discussion, perhaps in an appendix. What are the less accurate methods formerly used? How does the more accurate approach lead to better diagnostics? Provide a comparison to justify the “more accurate” characterization.
  We agree that we can be more specific here. We included a small historical review in Appendix B to discuss the improvements in the results (Fig. B1) and the computation (Fig. B2) and refer to it in Sect. 2.2.
  Manuscript changes: We removed the simplified lines 112-114: "This way of determining the corresponding temperature index is improved in precision compared to the previous versions, where the temperature index has been kept constant for all crossed isohalines." And added:
  - the line 107: ”We discuss the details of these changes more in Appendix B.”
  - **Appendix B : Development of the diathermohaline stream function computation**

- Line 64: “rotative” should be “rotational”
  Thank you. We changed it.

- Section 2.1: Throughout the formulation, the tacit assumption is that one is using a geopotential vertical coordinate (or the closely aligned z^* coordinate). But that choice is not ubiquitous. What about generalized vertical coordinates, such as used by MOM6 or even some cases with NEMO?
  This is a good point. In our study, all simulations are on z-/z^*-levels. But also for generalised vertical coordinates the computation of the stream function is valid since we evaluate the stream function in model levels. This means that the projection is independent on the vertical coordinate as long as the model output is stored in mass-/volume transports (preferable) and the mass/volume of the grid cells is given as a time dependent model output or the model layer thicknesses (in m) are stored as time dependent model output variables. Therefore, the formulation in the continuous form holds as well, independent of the model's vertical coordinates. We refer to this in Sect. 2.2 and in Sect. 3.4, when we discuss the model output variables, and in the concluding Sect. 7.
  Manuscript changes: We added:
  - the lines 112-113: "The implementation is independent of the model's vertical coordinate system, as long as the model layer thicknesses are given as time dependent model outputs (compare also Sect. 3.4)."
  - the lines 340-342: "[...] but want to stress that, in order to apply this, the model needs to be run with z^*-coordinates."
  - the lines 495-496: "It is independent of the ocean models' vertical coordinate system as it's computation is based on model levels."

- Line 73: NEMO and most all modern ocean climate models use Conservative Temperature, Θ, rather than potential temperature, θ. Indeed, as you already note in the caption to Figure 2 that you use NEMO with the TEOS-10 equation of state. So please correct this statement on line 73.
  Thank you for pointing this out. We see that it would be beneficial to use conservative temperature and

absolute salinities. The model outputs that we use, are, however, potential temperature and practical salinity. Only the EC-Earth simulations provide absolute salinity as model output. We use the gsw-toolbox (McDougall and Barker, 2011) to convert those outputs to practical salinity for the purpose of having a comparable variable between the different simulations. We add this statement in Sect. 3.1 and also correct the statement in the caption of Fig. 2 where we use EOS-80 to compute the isopycnals to be consistent. Furthermore, we included the option into the implementation (v2026.2) to use the gsw-toolbox for converting practical salinity and absolute salinity as well as potential temperature and conservative temperature to make the code more flexible in model comparison projects where different salinities and temperatures might be stored from different modelling groups.
Manuscript changes: We

- changed caption of Fig. 2 to: "[...] The computation of σ isopycnals are done with the International Equation of State of Seawater - 1980 (EOS-80); [...]";
- And added the lines 287-291: "For all model data the output is analysed in potential temperature and practical salinity. All data provide practical salinity as model output except from the EC-Earth3-Veg simulations which contain absolute salinities. To create a variable that is comparable between all data sets we convert the absolute salinities into practical salinities using the Gibbs-SeaWater Oceanographic Toolbox (McDougall and Barker, 2011). To use the implementation flexible in model intercomparison projects we include this optional conversion."

- Equations (2a, 2b) are fine for a continuum expression. But what is the actual discrete algorithm used? Are the Dirac deltas converted to Heavisides divided by ΔS and $\Delta\Theta$? Please clarify.
Thank you for the comment. We included equations in the numerical implementation section (Sect. 2.2) to summarise mathematically our descriptive explanation.
Manuscript changes: We added

- the lines 134 - 139: "We summarise the projection as discrete equations for $\dot{S}_{m,l} = \dot{S}^{iso}_{m,l} + \dot{S}^{adv}_{m,l}$ with

$$\dot{S}^{iso}_{m,l} = \frac{1}{N}\sum_{n}^{N}\left[\sum_{i}^{I}\sum_{j}^{J}\sum_{k}^{K}\frac{1}{\Delta t}0.5\left(V^{n}_{i,j,k}+V^{n-1}_{i,j,k}\right)\mathrm{sgn}\left(\left\lfloor S^{n}_{i,j,k}\right\rfloor-\left\lfloor S^{n-1}_{i,j,k}\right\rfloor\right)\delta^{S}\left(S_m,S^{n}_{i,j,k},S^{n-1}_{i,j,k}\right)\right.$$
$$\left.\delta^{\theta}\left(\left\lfloor\theta^{n}_{i,j,k}+\left(S_m-S^{n}_{i,j,k}\right)\frac{\Delta\theta}{\Delta S}\right\rfloor-\theta_l\right)\right],$$

$$\begin{aligned}\dot{S}^{adv}_{m,l} = \frac{1}{N}\sum_{n}^{N}\Bigg[&\sum_{i}^{I}\sum_{j}^{J}\sum_{k}^{K}\dot{U}^{n}_{i,j,k}\,\delta^{S}\left(S_m,S_{i,j,k},S_{i-1,j,k}\right)\delta^{\theta}\left(\left\lfloor\theta_{i,j,k}+\left(S_m-S_{i,j,k}\right)\frac{\Delta\theta}{\Delta S}\right\rfloor-\theta_l\right)\\&+\sum_{i}^{I}\sum_{j}^{J}\sum_{k}^{K}\dot{V}^{n}_{i,j,k}\,\delta^{S}\left(S_m,S_{i,j,k},S_{i,j-1,k}\right)\delta^{\theta}\left(\left\lfloor\theta_{i,j,k}+\left(S_m-S_{i,j,k}\right)\frac{\Delta\theta}{\Delta S}\right\rfloor-\theta_l\right)\\&+\sum_{i}^{I}\sum_{j}^{J}\sum_{k}^{K}\dot{W}^{n}_{i,j,k}\,\delta^{S}\left(S_m,S_{i,j,k},S_{i,j,k-1}\right)\delta^{\theta}\left(\left\lfloor\theta_{i,j,k}+\left(S_m-S_{i,j,k}\right)\frac{\Delta\theta}{\Delta S}\right\rfloor-\theta_l\right)\Bigg].\end{aligned}$$

with $\frac{\Delta\theta}{\Delta S}$ as the slope between the temperatures and salinities of two time steps of the same grid cell for $\dot{S}^{iso}_{m,l}$ or of the two neighboring grid cells for $\dot{S}^{adv}_{m,l}$ and

$$\delta^{S}\left(S_m,S_a,S_b\right)=\begin{cases}1 & S_m\in\left[\min\left(S_a,S_b\right),\max\left(S_a,S_b\right)\right]\\0 & \text{otherwise}\end{cases},\qquad \delta^{\theta}\left(\sigma\right)=\begin{cases}1 & \sigma=0\\0 & \sigma\neq 0\end{cases},\qquad sgn\left(\sigma\right)=\begin{cases}1 & \sigma>0\\0 & \sigma=0\\-1 & \sigma<0\end{cases},$$

and $\lfloor\sigma\rfloor$ bins σ and project them onto the largest isoline that is smaller than σ. $\dot{\theta}_{m,l} = \dot{\theta}^{iso}_{m,l} + \dot{\theta}^{adv}_{m,l}$ is computed equivalent."

- Line 90: “rational” should be “rotational”.
  Thank you. We changed it.

- For a non-simply connected domain, the Helmholtz decomposition (actually, the Helmholtz-Hodge decomposition) has a harmonic term that must be specified. See Denaro (2003) and Bhatia et al. (2013) for details. It is useful to here comment on the reason you drop the harmonic term. I suspect one can indeed ignore this term for global ψ and χ, yet it must be considered for basin diagnostics.
  Thank you for this comment. We added Bhatia et al. (2013) as reference and clarified this point in Sect. 2.1. Since we are not retrieving the rotational and divergent vector fields after computing the stream function and the potential, we are also not retrieving this vector component in our analysis.
  Manuscript changes: We added

  – the lines 100-102: "On finite domains, such as the thermohaline space, the vector field $\left(\dot{S}, \dot{\theta}\right)$, furthermore, incorporates an harmonic term which can be retrieved by subtracting the rotational and divergent components from the total vector field (Bhatia et al., 2013)."

- line 132: “convex hull” should be explained with a picture.
  We included a visualisation in panel e) of Appendix Fig. B1 and refer to it in section 2.2.
  Manuscript changes: We

  – changed the lines 142-143 to: "The applied boundary conditions are homogeneous Dirichlet Boundary Conditions ($\psi = \chi = 0$) on the convex hull of the thermohaline tendencies (shown in Appendix B1)."
  – added Panel e) in Appendix B1 .

- Line 133: I do not understand the need for “a small number of $\epsilon = 0.1$Sv on the boundary. Is that the geographic boundary? Watermass boundary? What is the need?
  We would like to thank you for this valuable comment and your critical questions. We wanted to restrict the stream function to a domain that focuses on the global thermohaline circulation. We agree that this is not an ideal way of handling the boundary in thermohaline space and that it restricts the domain too much. We now define the boundary of our computational domain where the thermohaline tendencies are zero which is more reasonable. This is changed to a new version of the code v2026.2 (Jung et al., 2026) and improved our comparison between the tendency potential with the fresh water fluxes at the sea surface in Sect. 2.4.
  Manuscript changes: We changed

  – the lines 142-143 to: "The applied boundary conditions are homogeneous Dirichlet Boundary Conditions ($\psi = \chi = 0$) on the convex hull of the thermohaline tendencies (shown in Appendix B1)."
  – Fig. 2, Fig. 3, Fig. 6, Fig. 7, Fig. 8, Fig. 9, Fig. 10, Fig. 11, Fig. A1 (changed to now Fig. A2), were updated using this updated boundary.
  – Small value updates in Sect. 5.1 and 5.2.

- Lines 137-138: provide some motivation for the choice of bin sizes. What are the ideas to consider by the diagnostician?
  To acknowledge this question, we extended the resolution study in the Appendix Fig. A1 by decreasing the resolution of the tracer space gradually and referred to it in section 2.2.
  Manuscript changes: We added

  – the lines 149-150: "We provide a small resolution study in the Appendix A, where we decrease the resolution in in tracer space. It can be seen that the resolution of 0.04psu and 0.16°C would have been sufficient but decreasing the resolution further would affect the solution. Please note, that the needed resolution might change in case other tracers are used and it is therefore recommended to verify in a similar resolution study whether the solution is robust to the chosen resolution."

- **Appendix A: Sensitivity of the stream function with resolution of the thermohaline space**

- Figure 3 caption: "back and grey" should be "black and grey".
  Thank you. We changed it.

- Line 216: My understanding is that NEMO conserves volume and tracer content to within computer roundoff. So I am puzzled with the phrase "and imperfect ocean mass conservation." Indeed, on line 238 you state "The model conserves volume". Please explain.
  Thank you for the comment. With imperfect ocean mass conservation we refer to the freshwater flux through the sea surface which we are investigating in this section. We understand that our formulation is confusing since we talk about the numerics of models in the same sentence. We changed the formulation.
  Manuscript changes: We changed
  - the lines 229-231 to: They discuss the tendency potential as a consequence of trends in salinity and temperature due to forcing, variability, model errors, and water mass exchange through the sea surface. Here, we compare the net sinks and sources from freshwater fluxes across the oceans' boundaries to the tendency potential.

- Line 255-256: provide more explanation for "contain the subgrid-scale diffusive parameterisations as part of the advective velocities". I do not wish to go to Wilson et al (2021) to see what you mean. This is a basic point for diagnosticians so you should provide an explanation here.
  We see that this formulation is confusing and remove it. What we mean is that ORCA12 does not have a mesoscale eddy parametrisation so that component is already "included" in the u,v in the output. But this is said already in the sentence before and raising the term "diffusion" is misleading.
  Manuscript changes: We
  - removed the lines 254-256: "NEMO in the 1/12° resolution contains no parametrisations for the lateral mixing due to eddies since it is eddy-resolving in most parts of the ocean (Bacon et al., 2015). Thus, the OGCM-1/12° data, contain the subgrid-scale diffusive parametrisations as part of the advective velocities (Wilson et al., 2021)."
  - removed the lines 264-265: "The OGCM-1/12° and GLORYS12 data are "eddy-rich" and thus contain the mesoscale eddy transports as part of the advective velocities (Wilson et al., 2021)."
  - added the lines 276-280: "All NEMO data sets used here (OGCM simulations, EC-Earth3-Veg and GLORYS12) use a turbulent kinetic energy (TKE) closure model for vertical eddy viscosity and diffusivity. The ORCA12 configurations (OGCM-1/12° and GLORYS12) contain no parametrisations for mesoscale eddies since it is eddy-resolving in most parts of the ocean (e.g. Bacon et al., 2015). Both ORCA1 configurations (EC-Earth3-Veg and OGCM-1°) use the Gent-McWilliams parametrisation (Gent and Mcwilliams, 1990) of mesoscale eddy-induced turbulence for the horizontal tracer diffusion (Treguier et al., 1997)."

- line 258: "the the"
  Thank you. We changed it.

- line 267-268: I am unsure what you are talking about here. Please be more precise.
  Unfortunately, the eddy induced velocities are not available from this simulation. To address this problem, we conducted a validation simulation using EC-Earth3-Veg where we store the Eulerian mean velocities as well as the eddy-induced velocities and also the volume transports to investigate their contribution. We added this clarification at this point of the manuscript and refer to the sensitivity test shown in Sect. 4.
  Manuscript changes: We

  - added the lines 281-284: "[...] They are included in the volume transports of the EC-Earth3-Veg and are not available from the OGCM-1°simulation. We therefore conduct a sensitivity study how much this velocity component is contributing to the stream function for the NEMO3.6 model of 1° horizontal resolution by analysing an EC-Earth3-Veg validation simulation for a pre-industrial time period of 10 years in Sect. 4."

- line 285: “the the”
  Thank you. We changed it.
- Figure 4 is lower quality than some of the others, such as Figure 1. Perhaps resolution is too low.
  We increased the resolution.
- line 324: ”for in the NEMO” should read “for the NEMO”
  Thank you. We changed it.
- line 326: “Reynold” should be ”Reynolds”
  Thank you. We changed it.
- line 336: “date” should be ”data”
  Thank you. We changed it.
- equation (7): avoid a line break after equation (7) to avoid having LATEXproduce an indentation.
  Thank you. We changed it.

Appendix A: Sensitivity of the stream function with resolution of the thermohaline space

Throughout this work we use a discretisation of the thermohaline space with 500 bins in both the temperature and the salinity axis which corresponds to a resolution of 0.02 psu and 0.08 °C. Comparing panel a) of Fig. 9, panel c) of Fig. A2, and panel a) of Fig. A1, we argue that a resolution of 0.04 psu and 0.16 °C would be still sufficient to represent the diathermohaline stream function. Decreasing the resolution further would lead in a loss of accuracy. We recommend a similar resolution study if stream function in other tracer spaces are computed. Figure A2 shows that the diathermohaline stream function is robust in a deviation from a equally bin numbers in both tracer axes. The tendency potential is, however, more sensitive which may be further investigated.

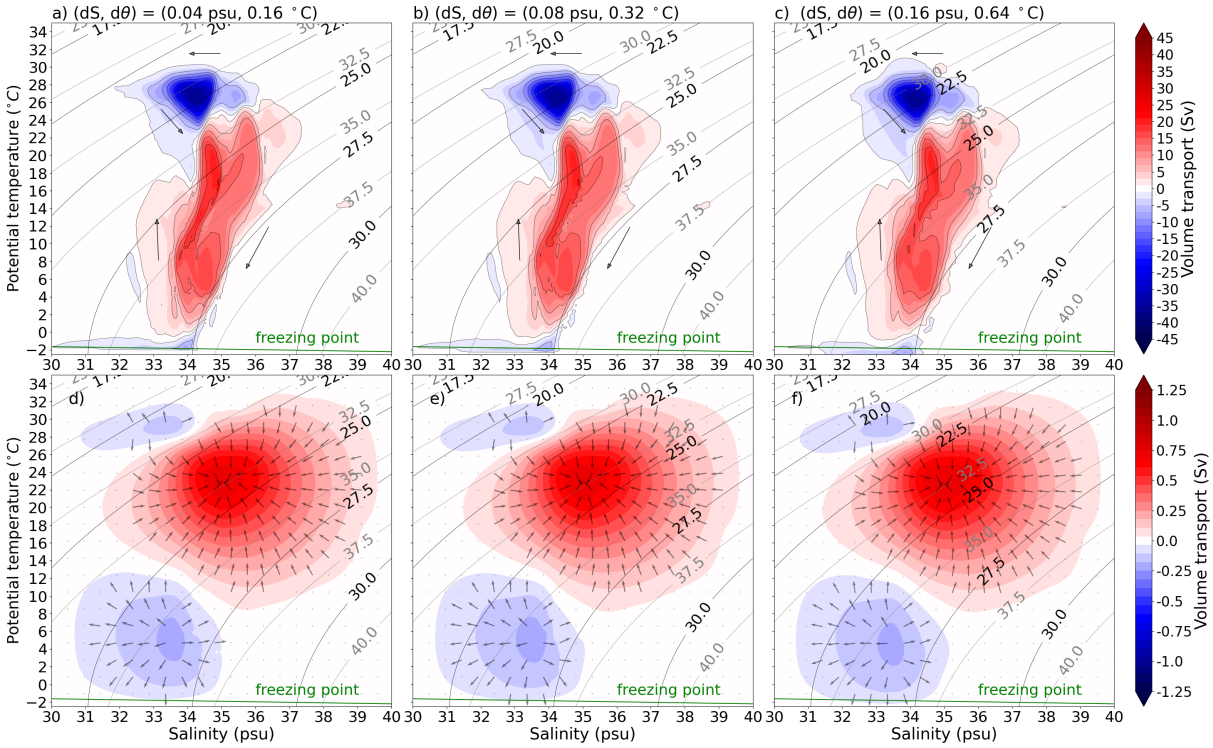


Figure A1: Sensitivity of the stream function ψ and the tendency potential χ of the ECEarth3-Veg PI simulation to the resolution of the tracer space with a decreasing resolution from panel a) to c) in both temperature and salinity. Isopycnals σ_0 and σ_2 are labelled in black and grey respectively $\left(\mathrm{kg\,m^{-3}}\right)$.

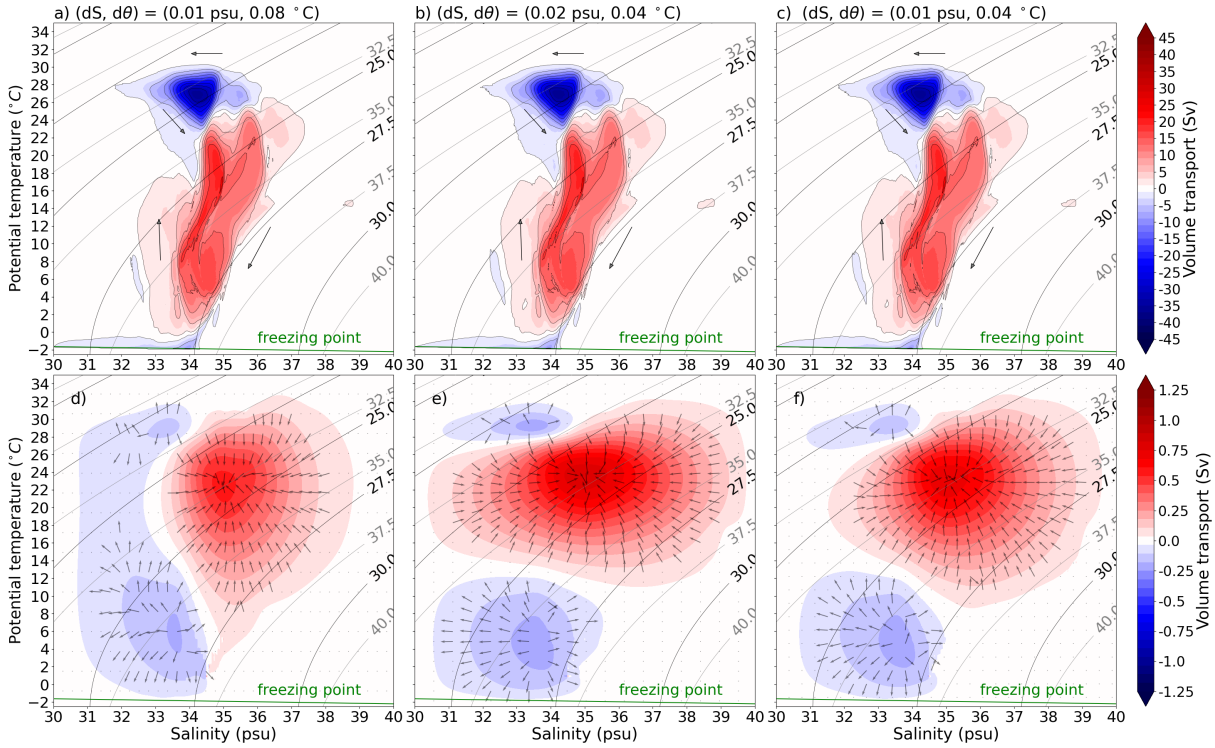


Figure A2: Sensitivity of the stream function ψ and the tendency potential χ of the ECEarth3-Veg PI simulation to deviation of the tracer space from a rectangular computation domain. Panel a) with decreased resolution in potential temperature, b) in salinity and c) both temperature and salinity. Isopycnals σ_0 and σ_2 are labelled in black and grey respectively $\left(\mathrm{kg\,m^{-3}}\right)$.

Appendix B: Development of the diathermohaline stream function computation

Figure B1 shows the development process of the diathermohaline stream function. Firstly, it was computed by integration of the advective components of the diahaline fluxes along the temperature axis or of the advective components of the diathermal fluxes along the salinity axis (panel a); compare for details Döös et al. (2012)). Thereafter, the partial derivatives of the temperatures and salinities with respect to time where included (panel b); compare Kjellsson et al. (2014) or Groeskamp et al. (2014) for details). This strengthened the magnitude of the stream function cells. In both versions, the temperature index of the diahaline tendencies and the salinity index of the diathermal tendencies where kept as a constant for all isolines that are crossed (compare panel a) in Fig B2). In Döös et al. (2017), the stream function was computed by applying a Helmholtz decomposition to separate divergent and non-divergent components of the vector field in thermohaline space. The Poisson equations where solved on a rectangular domain that was used for determining the vector field of the thermohaline tendencies $[S_{min}, S_{max}]\,[T_{min}, T_{max}] = [30, 40]\,[-3, 37]$. Furthermore, the projection was changed such that the temperature indices of the diahaline tendencies and the indices of the diathermal tendencies varied with a linear approximation (compare panel b) in Fig. B2). Here, the salinities and temperatures of the grid cells were first projected onto the nearest tracer indices, before $\Delta\theta/\Delta S$ was computed to then identify the corresponding temperature indices to project the volume flux to the discrete diahaline tendencies $\dot{S}_{m-1,l+1}$, $\dot{S}_{m,l}$ and $\dot{S}_{m+1,l}$.

In the current version, $\Delta\theta/\Delta S$ is computed by the actual temperatures and salinities of the grid cells which is then used to identify the corresponding temperature indices of the diahaline tendencies. This ensures that the volume flux is added to the actually crossed salinity indices (S_m, S_{m+1} and S_{m+2} instead of S_{m-1}, S_m and S_{m+1}) and leads to a better estimation of the corresponding temperature indices (e.g. $\dot{S}_{m+1,l-1}$

instead of $\dot{S}_{m+1,l}$). This improvement in precision is removing some fine structures mainly in the tendency potential and allows for a comparison with the net freshwater fluxes through the sea surface (compare Sect. 2.4). Furthermore, we exclude those areas of the thermohaline space from the computational domain, where the thermohaline tendencies are zero (shown in panel e) in Fig. B1).

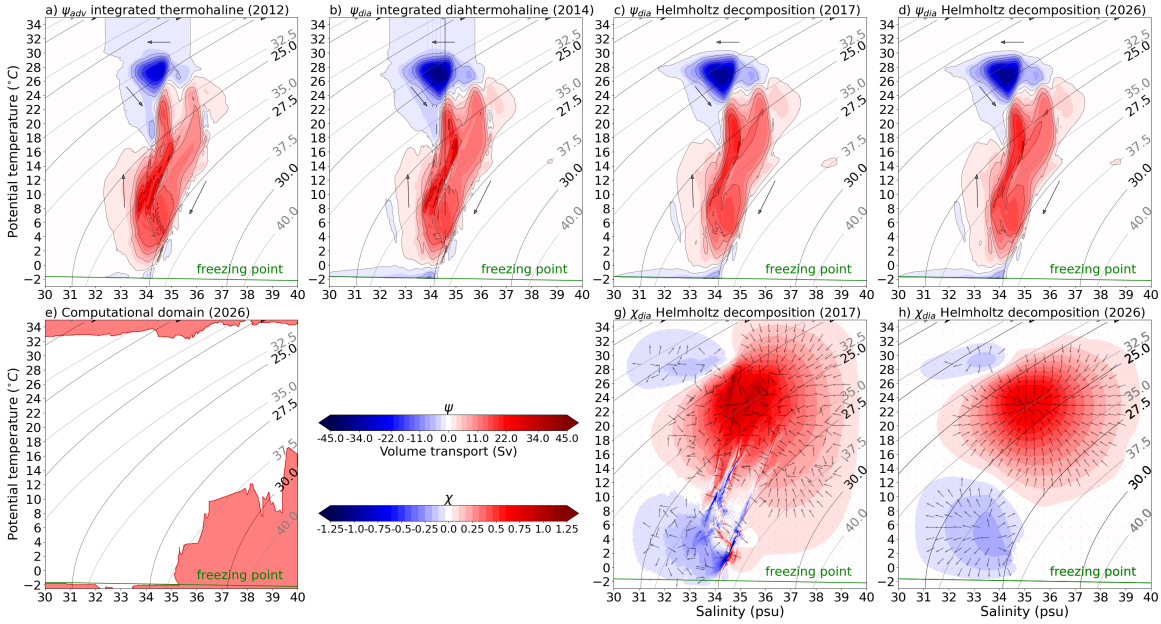


Figure B1: Development process of the diathermohaline stream function compuatation with a) the advective thermohaline stream function (Döös et al., 2012) that is based on integration and the projection shown in panel a) in B2, and b) the diathermohaline stream function (Kjellsson et al., 2014) build on integration and the projection shown in panel a) in B2, and panels c) and g) the diathermohaline stream function ψ_{dia} and the corresponding tendency potential χ_{dia} used in Döös et al. (2017) that is build on Helmholtz decomposition with a rectangular domain $[S_{min}, S_{max}]\,[T_{min}, T_{max}] = [30, 40]\,[-3, 37]$ and on a projection from physical to tracer space according to panel b) in Fig. B2. Panels d) and h) show the current version that is build on Helmholtz decomposition with a the domain where the thermohaline tendencies are zero, shown in panel e), and on a projection from physical to tracer space according to panel c) in Fig. B2.

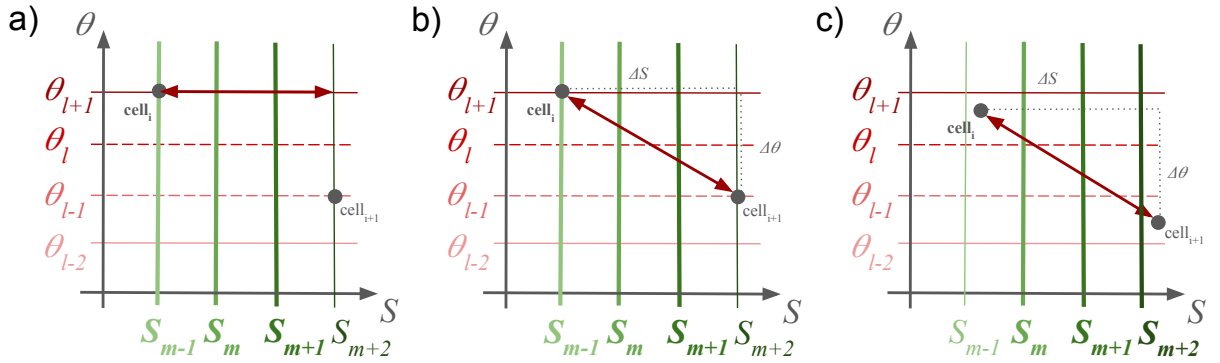


Figure B2: Visualisation of the methods evolution to determining the indices during the projection from physical space to thermohaline space on the example of the diahaline tendencies of panel a) in Fig. 1. Panel a) was used by e.g. Döös et al. (2017); Kjellsson et al. (2014) with the solutions that are shown in panel a) and b) in Fig. B1. Here, the tracer values of the grid cells were first projected onto the nearest discrete temperatures and salinities and the diahaline tendencies were added to salinity indices while the temperature index was kept constant ($\dot{S}_{m-1,l+1}$, $\dot{S}_{m,l+1}$ and $\dot{S}_{m+1,l+1}$). Panel b) shows the projection that was used e.g. in Döös et al. (2017) with the solutions in panels c) and d) in Fig. B1. Panel c) shows the current version which is explained in Fig. 1 with solutions in panels c) and d) in Fig. 6.

References

Bacon, S., Aksenov, Y., Fawcett, S., and Madec, G.: Arctic mass, freshwater and heat fluxes: methods and modelled seasonal variability, Philosophical Transactions of the Royal Society A: Mathematical, Physical and Engineering Sciences, 373, 20140 169, 10.1098/rsta.2014.0169, 2015.

Bhatia, H., Norgard, G., Pascucci, V., and Bremer, P.-T.: The Helmholtz-Hodge Decomposition—A Survey, IEEE Transactions on Visualization and Computer Graphics, 19, 1386–1404, 10.1109/TVCG.2012.316, 2013.

Döös, K., Nilsson, J., Nycander, J., Brodeau, L., and Ballarotta, M.: The World Ocean Thermohaline Circulation, Journal of Physical Oceanography, 42, 1445–1460, 10.1175/JPO-D-11-0163.1, 2012.

Döös, K., Kjellsson, J., Zika, J., Laliberté, F., Brodeau, L., and Campino, A. A.: The Coupled Ocean–Atmosphere Hydrothermohaline Circulation, Journal of Climate, 30, 631–647, 10.1175/JCLI-D -15-0759.1, 2017.

Gent, P. R. and Mcwilliams, J. C.: Isopycnal Mixing in Ocean Circulation Models, Journal of Physical Oceanography, 20, 150–155, 10.1175/1520-0485(1990)020<0150:IMIOCM>2.0.CO;2, 1990.

Groeskamp, S., Zika, J. D., McDougall, T. J., Sloyan, B. M., and Laliberté, F.: The Representation of Ocean Circulation and Variability in Thermodynamic Coordinates, Journal of Physical Oceanography, 44, 1735–1750, 10.1175/JPO-D-13-0213.1, 2014.

Jung, V., Aldama-Campino, A., Kjellsson, J., and Döös, K.: The diathermohaline stream function method (v2026.2), Zenodo [code and data set], https://doi.org/10.5281/zenodo.24600786, 2026.

Kjellsson, J., Döös, K., Laliberté, F. B., and Zika, J. D.: The Atmospheric General Circulation in Thermodynamical Coordinates, Journal of the Atmospheric Sciences, 71, 916–928, 10.1175/JAS-D-13-0173.1, 2014.

McDougall, T. and Barker, P.: Getting started with TEOS-10 and the Gibbs Seawater (GSW) Oceanographic Toolbox, SCOR/IAPSO WG, 127, 1–28, 2011.

Treguier, A. M., Held, I. M., and Larichev, V. D.: Parameterization of Quasigeostrophic Eddies in Primitive Equation Ocean Models, Journal of Physical Oceanography, 27, 567–580, 10.1175/1520-0485(1997)027<0567:POQEIP>2.0.CO;2, 1997.

Wilson, C., Aksenov, Y., Rynders, S., Kelly, S. J., Krumpen, T., and Coward, A. C.: Significant variability of structure and predictability of Arctic Ocean surface pathways affects basin-wide connectivity, Communications Earth & Environment, 2, 164, 10.1038/s43247-021-00237-0, 2021.

Zhang, R. and Thomas, M.: Horizontal circulation across density surfaces contributes substantially to the long-term mean northern Atlantic Meridional Overturning Circulation, Communications Earth & Environment, 2, 112, 10.1038/s43247-021-00182-y, 2021.